CRYSTAL Research & Technology

Cryst. Res. Technol. 52, No. 1, 1600171 (2017) / DOI 10.1002/crat.201600171

Review Article

Dislocation patterning and bunching in crystals and epitaxial layers - a review

*Peter Rudolph**

Received 12 June 2016, revised 16 August 2016, accepted 24 August 2016
Published online 16 September 2016

Cellular patterning and dislocation bundling as structures of dislocation dynamics in as-grown crystals and epitaxial layers are reviewed. Selected examples of multicrystalline (mc) silicon, III-V and II-VI compounds are presented. The origins of often overlaid dislocation networks varying by the cell scale and cell wall design are reported. The introduction in selected phenomenological fundamentals shows that dynamical polygonization basing on dislocation glide cannot be the only possible formation process. Even at high temperatures the point defect assisted climb plays a decisional role in the dislocation dynamics. Dissipative structuring via non-equilibrium thermodynamics is considered. Reduction of thermo-mechanical stress and control of stoichiometry are practical counter measures. Special attention is paid to the dislocation banding and their pile-up at grain boundaries leading to dislocation bunching. On the other hand at heteroepitaxial processes the controlled banding of dislocations is used to grow out them laterally. Further, second phase inclusions are responsible for dislocation accumulations. Their incorporation must be avoided by good mixing of the fluid phase and composition control. The required bridge intensification between crystal growers and metal physicists as well as the need of in situ experiments and advanced numeric modeling is underlined.

1 General introductory remarks

Dislocations are present in bulk crystals except of high-quality silicon, germanium, few organic and dielectric samples. Also epitaxial layers show this defect type due to the lattice misfit and differing thermal expansion between growing layer and substrate. As it is well known dislocations affect decisively the crystal and thin film parameters and, thus, the quality of devices made from. Therefore, since the beginning of productive crystal growth and epitaxy one of the key challenges for the crystal growers proves to be the reduction and even prevention of dislocations. But the efforts are accompanied by certain principal problems. At bulk growth the dislocation generation and multiplication is closely linked to inevitable thermo-mechanical stresses within the growing crystal caused by the interaction between required temperature gradients and crystal geometry that leads to characteristic inhomogeneous temperature distributions. In epitaxial systems the dislocation appearance is mainly attributed to the quasi unalterable compositionally induced mechanical stress situation. Thus, in most single crystalline crystals and epitaxial layers dislocations can be never avoided completely.[1] Further, the presented dislocations do not remain in a homogeneous arrangement but rather tend to form specific patterns and clusters, such as *cellular structures* and features of *bunching* (bundles, gnarls, tangles, veins), conflicting markedly with aimed parameter uniformity. Such situation results in the special task of *dislocation engineering* implying apart from dislocation minimization the control of their arrangement as homogeneous as possible. In fact, a homogeneous dislocation distribution without any patterning along a crystal wafer or epitaxial layer would reduce the parameter variation and, hence, the possibility of device failure. For instance, in crystals for optical applications dislocation cell structures cause light scattering due to the characteristic lattice orientation discontinuities between the cells. In semiconductor wafers and epitaxial layers such patterns

* Corresponding author: e-mail: rudolph@ctc-berlin.de, Phone: +49 3379 444253
Crystal Technology Consulting, Helga-Hahnemann-Str. 57, D-12529 Schönefeld, Germany

[1] Note, meanwhile during the growth of thin layers it may be possible to bend threading dislocation and enforce their lateral growing out. However, such measure leaves a marked density gradient along the layer thickness being mostly responsible for new stress generation.

CRYSTAL Research & Technology

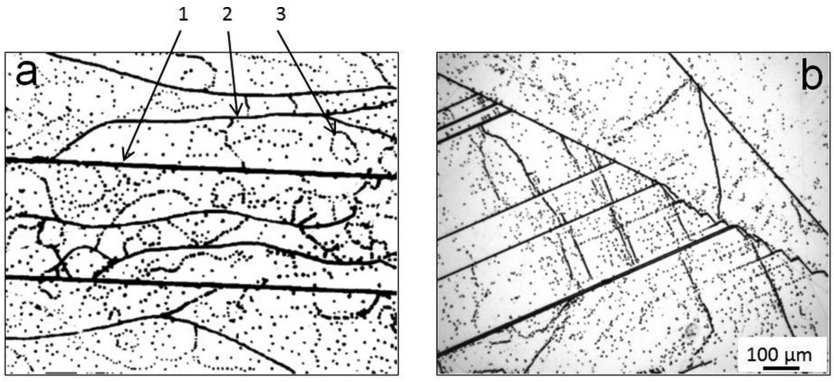

Fig. 1 a - Scheme of the sub grain structure of melt-grown crystals after Tsivinsky and Maslova published in CRT in 1980 [2], divided by the authors into 1. Macrosub-grains, 2. Microsubgrains, and 3. Minimum misorientation subgrains. b - current image of dislocation structures in mc-Si (curtesy from 2014 of T. Ervik, Norwegian University of Science and Technology).

produce mesocscopically inhomogeneous intrinsic and extrinsic point defect distribution that vary the resistivity and impede the electron transport. Dislocation bundles prove to be very harmful heterogeneous regions which markedly reduce the carrier lifetime and may produce short-circuits.

The features of dislocation patterning in as-grown crystals are well known since a long time. First images of electron microscopy during the fifties and sixties revealed the presence of characteristic cellular structures in metals, semiconductors and dielectrics very obviously. Primarily, they were solely attributed to the phenomenon of *dynamic polygonization (DP)* taking place during the cooling process of as-grown single crystals with stored thermomechanical stress. However, it soon became apparent that DP cannot be the only possible formation process. In many dislocation arrays cell walls made of many tangled dislocations have been observed which contradict the typical DP grain boundaries consisting of well-aligned single dislocation rows of identical Burgers vector. Furthermore, often an overlay of more dislocation nets varying by the cell scale is ascertained. In fact, in many crystalline samples the low-angle grain structure with well-pronounced sharp walls and larger cells up to millimetres is underlain by a substructure with much smaller, often not yet completed cells of some micrometre size. Whereas the first feature is formed by characteristic dislocation glide processes the second one occurs due to the very stress-sensitive interaction dynamics between glide and climb. Such point-defect-assisted formation of an array of misoriented cells takes place at elevated temperature and is sometimes named *static polygonization (SP)* somewhat confusing the really proceeding vehement kinetics. In principle, this type of cellular structures meets to a high degree the features of *dissipative structuring* via irreversible thermodynamics.

By comparison, dislocation bundles are mainly clustered at concave shaped interface regions and by dislocation pile-ups at grain boundaries. Very often they are also nucleated at second-phase particles (inclusions) within the crystal matrix. Parallel dislocation agglomerations can also start at crystal or wafer edges releasing thermo-mechanical stress by dislocation glide down to relatively low temperatures. Mostly they are nucleated as half-loops at surface irregularities at the crystal or wafer periphery.

In "Kristall und Technik (KT)", the precursor of the today "Crystal Research & Technology (CRT)", the earliest papers referring to various dislocation arrays in as-grown single crystals were published by Myshlyaev [1] and Tsivinsky and Maslova [2] in 1979 and 1980, respectively. The authors of ref. [2] classified all until then related and own observations in three grain categories differing in size and misorientation, in particular, macrosubgrains, microsubgrains and minimum misorientation subgrains as sketched in figure 1a. A nearly consistent newer image from a directionally solidified multicrystalline (mc) silicon ingot is shown in figure 1b. After Tsivinsky and Maslova the macrosubgrains are formed by the process of poligonization. Minimum misorientation subgrains were correlated with dislocation density and acting thermomechanical stress level. Microsubgrains were compared with dislocation linages, a type of bunching. Unfortunately, the role of intrinsic point defects was not considered yet. In contrast, at the same time Dashevsky and Eidenson [3] referred to the important role of impurities which can markedly contribute to the inhibition of cell structuring due to increasing critical resolved shear stress (CRSS) for dislocation mobility. Later, the highly interested situation of correlation between grain boundaries and dislocation mobility in mc-Si ingots for photovoltaics was reported by Schmid et al. [4]. Finally, the author of the present paper published a review on cellular structuring in growing crystals in 2005 [5]. As one can see during the whole of its first fifty years KT/CRT provided an useful contribution towards clarifying of these quite

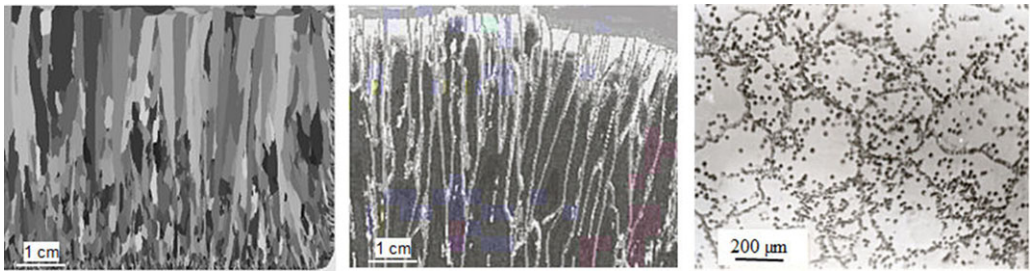

Fig. 2 Grain structures. Left – randomly nucleated polycrystalline structure of mc-Si; middle – elongated grain structure due to morphologically instable interface in a mc-Si crystal; right – cellular structure in a CdTe crystal (adapted images from refs. [6, 7 and 5], respectively).

complex effects of *dislocation dynamics (DD)* in as-grown crystals.

It is important to differ between three totally different reasons of generation of grain structures during a crystallization process (figure 2). Firstly, at *random nucleation* multicrystalline growth is induced that leads to a well-pronounced grain growth with misorientation angles of some degrees [6]. Note, also at epitaxial lateral overgrowth (ELOG) after the evenly spreaded nucleation the coalesced areas show characteristic tilt angles which are, however, much smaller in the region of some dozens arc sec only, due to the well-oriented nucleation assisting template patterns. Then, in bulk crystals sometimes an elongated grain structure parallel to the growth direction can be obtained [7]. Such feature is mostly caused by a cellular-shaped melt-solid interface forced to *morphological instability* due to constitutional supercooling. The tilt angle of such configuration can reach some arc minutes. Finally, *stress-induced dislocation patterning* with tilt angles in the range from arc seconds to arc minutes can be obtained [5]. Only this category is reviewed in the present paper. Of course, there is an enormous number of publications on cellular structuring under mechanical load (rolling, bending, indention) belonging to the branches of material science and metal physics from which, however, the crystal grower can still learn much more than before. A related fundamental compendium was recently published by Kubin [8].

2 Selected phenomenological fundamentals

To understand the interaction forces between dislocations as essential prerequisite for dislocation pattern formation the following background relations are comprehensively summarized (a more profound treatment of DD is given by Amodeo and Ghoniem [9]). As it is well known, the atoms in a crystal containing a dislocation are displaced from their perfect lattice sites, and the resulting distortion produces a stress field around the dislocation. Thus, each single dislocation is a source of internal stress within the crystal contributing to its enthalpy outside of the thermodynamical equilibrium. The created *elastic energy* of single screw ($\kappa = 1$) and edge ($\kappa = 1 - \mu$) dislocation is

$$E_s = (Gb^2/4\pi\kappa) \ln (R/r_o) \quad (1)$$

with G - shear modulus, b - Burgers vector, μ - Poisson ratio, R - crystal radius and r_o - radius of dislocation core $\sim 5b$, the region where the displacement field around the dislocation is not more accurately described by linear elasticity. Recently was shown by molecular dynamic (MD) simulations that even in the center the maximum local stress can reach values up to GPa [10]. Although the exponential drop of E_s outside the core a sufficiently significant long-range force on each another presented dislocation is still acting that depends on the mean dislocation distance $\lambda = \rho^{-1/2}$ (ρ - dislocation density). Then the total force on a given dislocation can be computed by summing the individual long-range forces resulting from all other dislocations as Peach-Koehler [11] relation. That means, within the crystal a reciprocal energetically driving force between all presented dislocations take place aimed on common crystal enthalpy reduction. Indeed, the dislocations are subjected to a *screening effect* reducing their single elastic energy with increasing dislocation density, i.e. decreasing distance between them. Thus, an infinitesimal displacement of a given dislocation within a primary homogeneous dislocation arrangement towards another dislocation enhances its energetical screening and is, therefore, thermodynamically favoured. This effect is additionally supported when external forces, such as thermo-mechanical stress, are attacking. Then the stress-induced Peach-Koehler force on the dislocation is

$$F = b\sigma(r, \theta) \quad (2)$$

with b - Burgers vector, $\sigma(r,\theta)$ - acting stress in cylindrical coordinates. Projecting F onto a direction within the

glide plane becomes the glide force $F_{gl} = Ff_s$ with the Schmidt factor $f_s = \cos\alpha \cos\beta$ where α and β are the angles between stress and normal to the glide plane and stress direction, respectively. The resolved shear stress on the gliding dislocation is then

$$\tau_g = F_{gl}/b = \sigma(r,\theta)\, f_s \tag{3}$$

Thus, the stored dislocations of a crystal under acting thermo-mechanical stress are subjected to *glide* whose two-dimensionality is supplemented by three-dimensional (3D) processes like point-defect assisted *climb* and *cross slip* leading in ensemble to spatial structural patterning [5]. The velocities by glide v_g and climb v_c are given by the relations

$$v_g = v_o(\tau_{eff})^m \exp(-E_a/kT) \tag{4a}$$

$$v_c = v_o(\tau_{eff})^{Nc} \exp(-E_{SD}/kT) \tag{4b}$$

with v_o - material constant, τ_{eff} - effective shear stress on dislocation, m - stress exponent, E_a -activation energy (Peierls barrier), k - Boltzmann constant, T - absolute temperature, N_c - climb exponent correlating with point defect diffusivity, E_{SD} - activation energy for given point defect diffusion. If the stress falls below the friction stress (Peierls barrier) the dislocation becomes immobilized but its elastic strain does still act on the other dislocations.

Important preconditions of difussion-assisied climb and cross slip are elevated temperature and relative high stacking fault energy, respectively. Even in semiconductor compounds with zinc blende structure containing characteristic partial dislocations (Shokley partials) cross-slip can be restrained due to a large equilibrium stacking fault distance between them being inversely related to the stacking fault energy γ_{SF} as

$$d_{Sh} = G\, a^2/(24\pi\gamma g_{SF}) \tag{5}$$

with G - shear modulus and a - the lattice parameter.

On their way of stress-driven displacement the dislocations are confronted with the following nonlinear interactions supporting the energy yield and patterning markedly.

Annihilation: the cancellation of two dislocations of opposite Burgers vectors b which approach each other along a given crystallographic plane. The critical distance for annihilation of two screw dislocations has been estimated to be $y_{cr} \approx Gb/2\pi\tau_g$ amounting in metals around 2 μm (note, the critical distance for edge dislocation annihilation has been found to be on the order of 1- 2 nm only) [7]. This process contributes to high gain of energy due to the destruction of energy-afflicted defects.

Dipole formation: two edge dislocations of opposite Burgers vectors gliding past each other on parallel slip planes tend to form stable dipole pairs reducing the elastic energy in dipole in comparison to the single dislocation energy. Their typical lengths are on the order of tenths of microns. Only edge dislocations can form dipoles since screw dislocations can easily annihilate by cross-slip. Usually, dipoles do not move as a whole but can change their configuration (angle between dislocations) in dependency on acting stress value [7]. At moderate friction stress below CRSS, i.e. at absence of dislocation multiplication, a stable configuration can be reached by the formation of self-screening multipolar clusters reflecting an island-like assembling of elementary dipols.

Wall formation: generally, dislocations of opposite Burgers vectors tend to annihilate and the residual ones of identical b accumulate in walls. Energetically, an array of edge dislocations of the same sign is most stable when the dislocations lie vertically above one another. The difference in energy, i.e. the gain, between single dislocations E_s and total energy of dislocation in a network of walls E_n is [12]:

$$E_s - E_n = \frac{1}{4}\frac{Gb^2}{\pi(1-\mu)}\rho \ln\frac{\lambda_w}{h_n} \tag{6}$$

with G - shear modulus, b - Burgers vector, μ - Poisson ratio, ρ - dislocation density, h_n - distance between dislocations in walls, λ_w - spacing between walls. A relation of E_n / $E_s \approx 0.25$ can be obtained proving to be an essential contribution to the crystal enthalpy reduction. In metal physics the dislocations stacked in such walls are named *geometrically necessary dislocations (GND)*. Such process plays a decisional role at dynamical polygonization. Figure 3 shows the simulation result of Gulluoglou et al. [13] when an initially random distribution of edge dislocations on parallel slip planes relaxes under the influence of their mutual interactions.

Junction formation: if two dislocations of identical Burgers vector approach each other they can lock together as Lomer-Cottrell barrier or form a jog intersection or intersect by passing each other. In result characteristic highly regular networks can be formed.

Dislocation multiplication: apart from cross slip which splits the dislocation in basic and slipped branches its multiplication can also taking place by pinning at two obstacles and bowing out in between. In result a annihilating loop is formed whereas the new dislocation line between the obstacles is subjected to

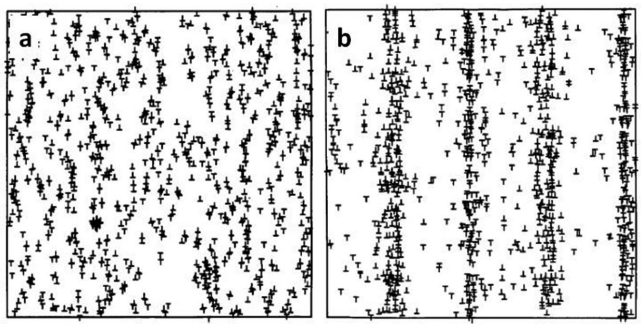

Fig. 3 Simulated relaxing wall patterning of edge dislocations. a - random starting distribution; b - periodic patterning of sharp walls with a distance to each other of 0.5 μm at which the elastic interactions are truncated (adapted from ref. [13]).

the same procedure named Frank-Read mechanism. Multiplication occurs when the acting shear stress τ exceeds the ratio Gb/L (L - interobstacle spacing).

Dislocation pile-up: when the leading dislocation of a migrating dislocation trail meets a barrier (grain boundary, inclusion, sessile dislocation cluster) and is stopped by it the following dislocations pile-up, but do not combine due to the same sign. As the result an enormous shear stress (up to GPa) is developing around the leading dislocation responsible for possible generation of new dislocations, dislocation bundles and sub-grain boundaries (cells) in order to minimize the dammed energy.

Dislocation bending: dislocations that meet crystal surfaces such as propagating fluid-solid interfaces experience forces not encountered in the bulk [14]. The dislocation is attracted towards a free surface where the material is more compliant and the dislocation energy is lower. Contrary, at rigid surface the dislocation is repelled. To treat this mathematically, the imaginary stress field of the given dislocation type is added. Such an *image dislocation* is a virtual dislocation situated outside the material, which generates a stress field compensating at the free surface the stress field of the actual inner dislocation. The image force has no effect, for symmetry reasons, on the dislocations when they are perpendicular to a basal surface. On the other hand, they move their lines in the basal plane when they become close enough to an inclined facet (figure 4a) [15]. The observed dislocation alignment perpendicularly to a growing interface plane has been also explained by the minimum-energy theorem [16] whereupon the dislocation lines adopt a direction l, for which its energy within any growth layer is a minimum. For a growth layer of unit thickness $d = 1$, this can be expressed as $E/\cos\alpha = \min$, with E the elastic (strain) energy per unit length of the dislocation line and α the angle between l and normal to the surface (figure 4b). Dislocation bending is of both unfavorable and favorable effect. First, it leads to harmful dislocation bunching in concave or reentrant angles of growing interface. Contrary to that it helps to grow out dislocations at convex interfaces. A high practical relevance proves to be in epitaxial processes. Adjusting an interim 3D growth mode of multi-pyramidal interface morphology original perpendicularly directed dislocation bend sideways towards pyramidal facets and can laterally annihilate and grow out (figure 4c) [17]. As a result the dislocation density is decreased along the crystal thickness.

Dissipative structuring: Principally, dislocations are metastable defects with high energy, their density cannot be drawn from equilibrium thermodynamics alone. The thermomechanical work done during plastic flow is mainly dissipated into heat and the rest is stored in form of elastic dislocation energy. Strictly speaking, such process is far from thermodynamic equilibrium and promotes spontaneous forms of self-organization, i.e. dissipative structures, such as periodic and cellular

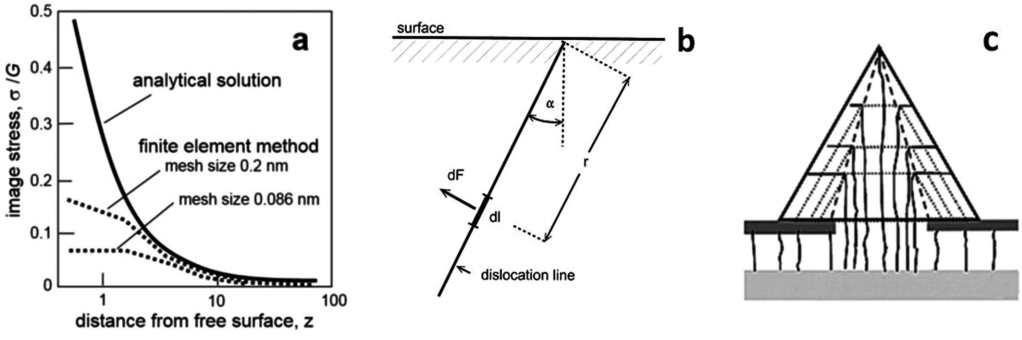

Fig. 4 a - calculation of the normed image stresses σ/G (G - shear modulus) along the dislocation line near to the free surface in a semi-infinite fcc medium; b - illustration of the force dF exerted by the crystal surface upon a line segment dl of a straight dislocation line emerging at the surface; c - sketched bowing of dislocations initially growing perpendicular through a mask window and then bended at the facets of overgrowing pyramids (adapted from refs. [15–17], respectively).

CRYSTAL Research&Technology

dislocation patterns [6]. Dislocation self-organization processes can also lead to slip localization and various non-uniform dislocation structures. Thus, formation of structures is closely correlated with the general spatial instability of dislocation distribution within the crystal resulting from dislocation immobilities at obstacles or as dipole configuration, for example, and their mutual energetic correlation producing dislocation flux and its fluctuation. The out-of-equilibrium situation induced to model dislocation patterning as a synergetic pattern formation phenomenon, in analogy with spatial structuring in many driven far-from-equilibrium systems (the principle of Glansdorff-Prigogine). The mathematical adaption to dislocation systems proves to be quite challenging and must be studied in the special literature (e.g. [6], [18], [19]). Here is given the general concept only.

The temporal evolution of dislocation pattern via elastic energy distribution within the crystal volume can be derived by the time evolution of ρ via the dislocation flux J

$$\partial\rho/\partial t = -\nabla J + f(\rho_1) \tag{7}$$

where J can be correlated to the gradient of average dislocation energy $\sim\nabla E/\mu$ (μ - friction coefficient) [15] or diffusivity $\sim\nabla D\rho_{\mathrm{m,i}}$ [20] and $f(\rho_{\mathrm{m,i}})$ is the non-linear reaction term implying the local interactions between dislocations by considering mobile (m) and immobile (i) dislocations. Setting the linear evolution equation for the fluctuation of mobile and immobile dislocation density in Fourier space $\rho_{\mathrm{m,i}} = \rho_{\mathrm{m,i}}{}^{\mathrm{o}} + \tilde{\rho}_{\mathrm{m,i}}$ ($\rho_{\mathrm{m,i}}{}^{\mathrm{o}}$ - steady-state starting density) one looks for the case of instability of the starting homogeneous steady-state equation (7) being equated with oscillatory temporal behavior leading to spatial pattering. As a result becomes the pattern wavelength λ of dislocation density fluctuations showing proportionality to the mean dislocation distance (i.e. via density) of the starting density as $\lambda \sim (\rho_{\mathrm{m,i}}{}^{\mathrm{o}})^{-1/2}$.

Dislocation density distribution - Nye tensor: as it was shown in the former section a strictly homogeneous dislocation distribution proves to be a quasi ideal situation that can be hardly realized due to its high energetical instability. We showed many processes supporting the reduction of elastic energy of a single dislocation in ensembles (e.g. dipoles, walls). However, markedly inhomogeneous dislocation configurations, e.g. bundles or clusters, can create a new strain contribution. This is of special importance in heteroepitaxial processes when dislocations are bundled artificially by using masks with periodical growth windows like at ELOG, for example. A tensorial function integrating the stress over all dislocations within a finite volume element V is given by the *Nye tensor* [21]

$$\alpha_{ij} = \frac{1}{V}\int b_i t_j ds \tag{8}$$

with b - Burgers vector, t - unit vector tangent to dislocation line l, ds - radian, and indices i, j - directions of b,l respectively. According the conditions of compatibility $\nabla \times \varepsilon_{xy} = \kappa_{st} - \alpha_{ij}$ with ε_{xy} - elastic stress tensor, κ_{st} - Stoney's bending curvature $\sim\sigma h_{\mathrm{l}}/h_{\mathrm{s}}{}^2$ (σ - acting layer stress, $h_{\mathrm{l,s}}$ - layer and substrate thickness, respectively), even if $\varepsilon_{xy} = 0$ a tensile bending can still obtained because κ is then exclusively determined by the Nye tensor ($\kappa \sim \alpha_{ij}$) which is greater then zero when an inhomogeneous dislocation distribution takes place. Usually, a concave epitaxial layer bending causes complications at subsequent technological steps and should be prevented as well as possible. But this seems to be the big challenge due to the typical DD inhomogeneities. Recently, Gorn et al. [22] simulated numerically the dislocation-induced stress in GaN films showing grain structure and found that the maximal values of stress components s_{xx}, s_{yy}, s_{zz} are rapidly reducing with decreasing grain diameter d. Due to the decreasing mean dislocation density with the epitaxial layer thickness h_{l} also a sensitive stress reduction along h_{l} was observed (see figure 10b).

To summarize the above collected DD processes in short it is obvious that dislocations presented in growing crystals within characteristic thermal and stress fields are subjected to collective patterning for two reasons, i.e. i) minimization of the individual dislocation energy by screening in ensemble and, thus, contributing to decrease of the crystal enthalpy, and ii) self-organization of dissipative structures due to continuous entropy production via thermal, diffusive and stress fluxes being typically for open systems out of thermodynamic equilibrium to which belongs, strictly speaking, each crystallization process.

Figure 5 summarizes important above listed DD processes having share at formation of dislocation patterning and bunching.

3 Experimental observations and counter actions

3.1 Dislocation cells

Cell patterning is studied best in metals under an external load, but also in post-deformed elemental and compound crystals. Today, there is a large number of

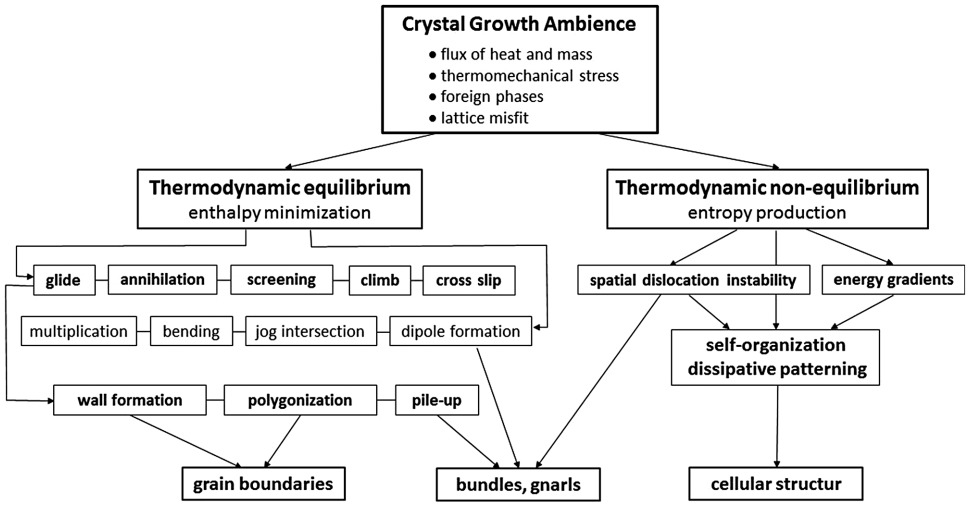

Fig. 5 Listing of important effects of dislocation dynamics generated under the crystal growth ambience by considering thermodynamical equilibrium and non-equilibrium principles. As can be seen both the wealth and complexity of acting processes complicate the finding out of clear hierarchical linkages reflecting the characteristic DD universalism. Note, the formation of regular dislocation networks (cross-hatchings) due to lattice misfit during heteroepitaxial processes are here not considered.

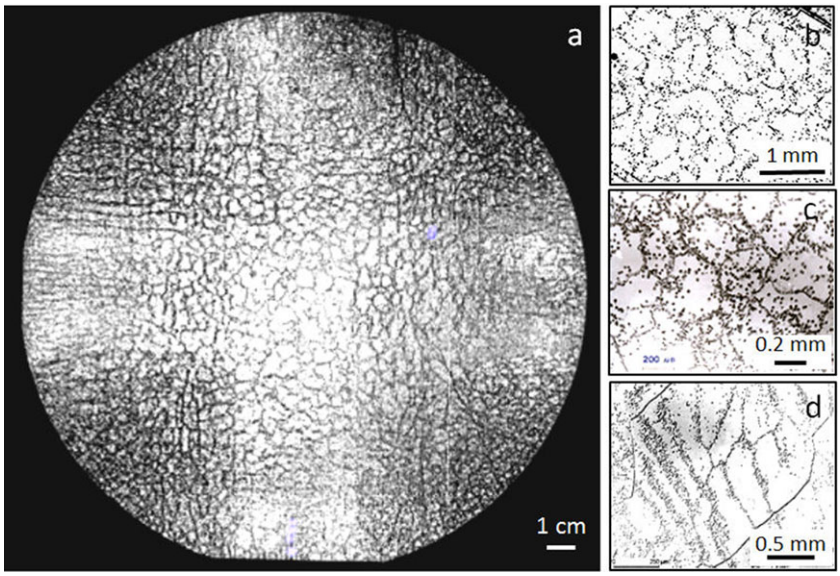

Fig. 6 Selected images of etched wafers with dislocation cell structures cut perpendicularly to the growth direction from various as-grown vertical gradient freeze (VGF) crystals. a - GaAs (courtesy of Freiberger CM from 2006), b - mc-Si (courtesy of G. Stokkan from 2012), c - $Cd_{0.96}Zn_{0.04}Te$, d - CaF_2 (c,d: author's collection).

papers dealing with, especially in the field of metal physics and mechanics (e.g. [6, 23]). Dislocation cells are also found in as-grown crystals, such as III-Vs, II-VIs, SiC, metals, dielectrics and mulicrystalline silicon ingots, independently which growth method was applied [5]. Figure 6 shows selected etched wafers cut from varous vertical gradient freeze (VGF) crystals. However, there is not yet a detailed knowledge about the proceeding DD within a growing crystal even at high temperatures. In all probability, cellular substructures are due to the acting internal thermomechanical stress field.

It can be assumed that 3D cell formation takes place immediately behind the propagating fluid-solid interface where the plastic relaxation by dislocation multiplication and the highest point defect diffusivity are obtained. For instance, there are well-confirmed in-situ analysis on crystallizing and remelting Al foils by Grange et al. [24] which observed by real-time synchrotron X-ray topography that the cellular dislocation structure appears due to the thermally induced strain within the region already some millimetres behind the melt-solid phase boundary. Jakobson et al. [25] confirmed such fast dynamics by in-situ X-ray reflection analysis on

CRYSTAL Research&Technology

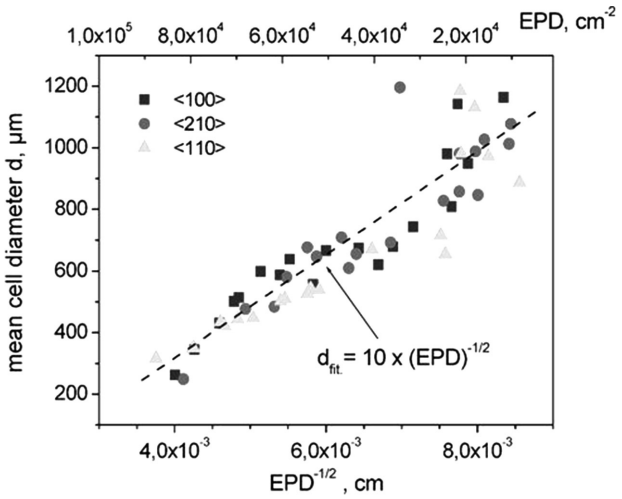

Fig. 7 Etch pit density (EPD) measurements of the cell diameter d on (100)-oriented wafers along crystallographic directions <100>, <210> and <111> vs. dislocation spacing $EPD^{-1/2} \approx \rho^{-1/2}$ (ρ - mean dislocation density) compiled from different GaAs crystals grown by liquid encapsulation Czochralski (LEC), vapour pressure controlled Czochralski (VCz) and VGF methods. The values $200 < d < 600$ μm and $500 < d < 1200$ μm belong to LEC/VCz and VGF, respectively.

deforming Cu crystals. The observation strongly indicated that the subgrain formation is initiated shortly after onset of plastic deformation. This result is of high importance for understanding the cell genesis in growing crystals whereupon the cell pattern in the cooled crystal can be assumed to be identical with the structure formed under high temperatures and is, therefore, generated by the initially acting thermo-elastic stress in synergy with point defect dynamics.

A systematic analysis of the origins and genesis of cell formation during the growth of single-crystalline semiconductor compounds, especially GaAs, was provided by the author and his former team [26–28]. First, the relation between the stored dislocation density ρ and the cell size (diameter) d has been determined. To deduce the 3D cell diameters from the 2D etch pit images, obtained on cut wafers, a stereological analysing method was used as described in ref. [28]. Figure 7 shows this correlation taken from experimental data. For GaAs samples with EPD $\geq 10^4$ cm^{-2} the mean cell diameter d correlates with dislocation density ρ as

$$d \approx K\rho^{-1/2} \tag{9}$$

with the factor of proportionality $K \approx 10$. Note the value $\rho^{-1/2}$ equates to the mean distance between not yet patterned dislocations. The result fits quite well Holt's scaling relations in deformed metals [29]. At dislocation densities below 5×10^3 cm^{-2}, however, the cells begin to dissociate.

Then, the relation between cell dimension and acting stress was investigated. In the case of growing crystals such analysis is more difficult due to the still impracticality of in situ measurement of the acting thermomechanical stress. Considering that the subgrain generation is initiated shortly after the onset of plastic deformation it can be assumed that the frontal elastic strain acting immediately after the propagating phase boundary can be assumed to be the driving force. This stress value is today readily calculable by global numeric modelling [30]. Therefore, we used the calculated frontal thermoelastic shear stresses of growth situations being identical with the real growth positions of each crystal from which the cell size measurements were taken. The data were inserted into the Kuhlmann-Wilsdorf relation

$$d = KGb\tau^{-1} \tag{10}$$

with G the shear modulus of Young, b the Burgers vector and τ the acting shear stress. The correlation between cell diameter d and τ^{-1} in the form of relation (10) shows figure 8. For comparison, the results from deformed GaAs, InP, metals as well as the slopes for NaCl and LiF are included [31]. As can be seen, for cell sizes smaller than 700 μm and calculated stresses larger than about 1 MPa the functional slope is similar to those of deformed materials. Independent of the growth conditions, it was found that d is inversely proportional to τ^{-1}. Obviously, in this region dislocation glide is the prevailing driving force for cell formation, due to the fact that the stress is larger than the critical resolved shear stress. In the case of larger cell dimensions, e.g. in VGF GaAs with dimensions of some mm within the centre (figure 6a), the $d(\tau)$ trend changes, showing smaller slope than -1. In these regions a resolved shear stress $\tau < 1$ MPa was calculated. One can suppose that for such very low thermomechanical stress, even below the critical resolved shear stress (GaAs: $\tau_{CRSS} \approx 0.5$ MPa), glide-driven plastic relaxation can no longer be the prevailing driving force for cell formation. Other cell structuring mechanisms must become dominant, like point-defect-controlled diffusive creep. No matter what kind of cell formation mechanism is taking place in detail the deeper-lying cause seems to be the self-organizing dissipative structuring within the acting thermal and stress flows as it was discussed in ch. 2.

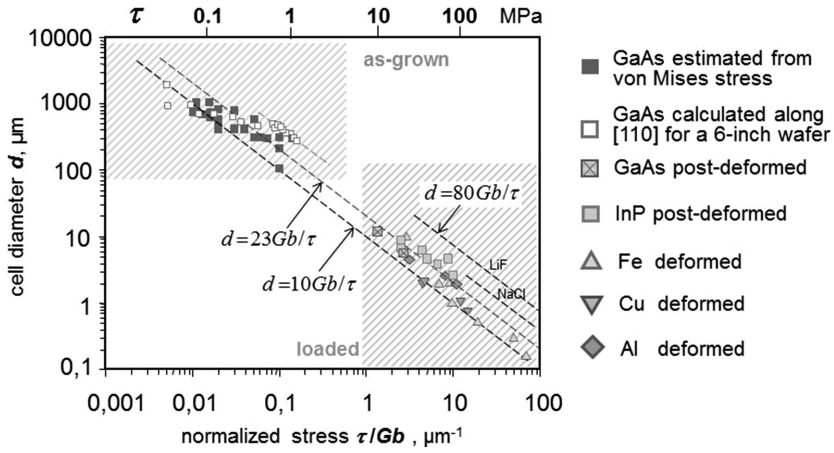

Fig. 8 Measured dislocation cell size d vs. calculated normalized resolved shear stress τ/Gb along the [110] direction of as-grown 6-inch VCz GaAs wafers in comparison with the data of post-deformed GaAs, InP and some metals. The slopes for some post-deformed NaCl and LiF are added (adapted from ref. [5]).

Finally, one can correlate the dislocation density with the acting stress via the Taylor relation

$$\tau = KGb\rho^{1/2} \tag{11}$$

Note, there is a long-term matter of debate about the correlation factor. Poirier [31] summarized that K has a value of about 10 for metals and 25 to 80 for ionic and oxide crystals. Recently Kubin pointed out that in metals the stress and cell size values should follow the similitude relation with a coefficient of $K \approx 7$ [8]. Concerning the author's analysis K ranges between 10 and 23 for semiconductor compound crystals (see figure 8).

Due to these "relations of similitude" (9) - (11) the crystal grower has a very good tool to correlate the measurable dislocation densities and cell sizes with the acting thermo-mechanical stress. For instance, in semiconductor materials a cell diameter of $\sim 100\ \mu$m requires a stress of about 1 MPa (see figure 8). Values of about 10 MPa are responsible for a cell diameter around 10 μm independently of which material is growing.

Usually, dislocation substructures impair the crystal quality. They cause refraction inhomogeneities in optical crystals. Across semi-insulating GaAs wafers, important for production of low-noise high-frequency devices, a mesoscopic resistivity variation does occur due to the accumulation of As_{Ga} antisite defects (EL2) within the cell walls. Subgrain boundaries impede also the electron transport in CdTe radiation detectors. Hence, the crystal grower is usually strived to find out proper measures to prevent dislocation patterning being, however, a great challenge. Hardly it is possible to overcome the universal principle of dissipative structuring as it was introduced in ch. 2.

Of course, substructuring can be damped first of all by adherence of the *lowest possible thermomechanical stress* during growth. Then, *solution hardening* proves to be an effective measure to reduce the dislocation mobility. For instance, no cells were found in CdTe and PbTe crystals when mixing components Se ($x > 0.4$) and Sn ($x > 0.15$) were added, respectively [5]. However, there is the well-known drawback of segregation when dopants are added to the melt. Further appears the danger of morphological interface instability by constitutional supercooling and, thus, low growth rates or high temperature gradients are required for its prevention.

Another possible way to prevent cell patterning is the minimization of the intrinsic point defect content by *in-situ control of stoichiometry* during growth. The stoichiometry is regulated by the partial pressure of the volatile component over the melt applying an extra heated source within the growth chamber (e.g. As or P at melt growth of GaAs or InP, respectively). The author's former team demonstrated by using a vapor pressure controlled Czochralski arrangement without boric oxide encapsulant that the cellular structure dissolves when the GaAs crystal is growing from proper controlled Ga-rich melt composition [32]. At near-stoichiometric growth the native point defect concentration and, thus, their contribution to the cell formation by climb (see ch. 2) is minimized. Bako et al. [33] confirmed this result theoretically by numeric calculations of cell patterning in a hexagonal lattice model with and without consideration of climb. In fact, if the dislocation climb is negligible compared to glide the dislocation configuration remains nearly random. When, however, dislocation climb is ''turned on'' a cell-like dislocation structure has been developed.

3.2 Sharp pronounced low-angle grain boundaries

Often the cell structure is superimposed by a low-angle grain structure consisting of much larger grain size with

CRYSTAL Research&Technology

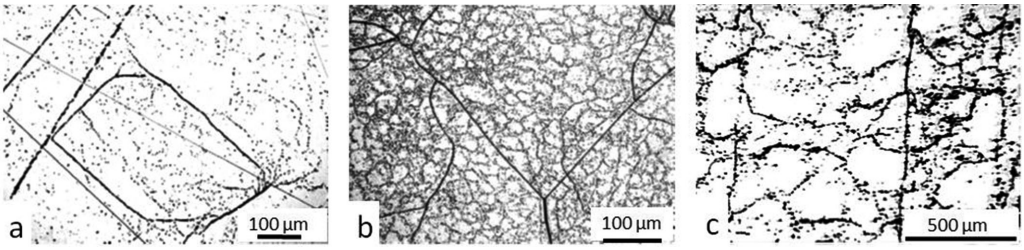

Fig. 9 Combined appearance of cell structure and superimposing low-angle grain structure consisting of much larger grain size with sharp and mostly straight aligned wall sections. a - mc-Si (adapted from ref. [34]; lines running through the image in various directions are surface scratches from the polishing procedure); b - at 843 K deformed NaCl single crystal (adapted from ref. [35]); c - vertical Bridgman-grown CdTe single crystal (author's collection).

sharp and mostly straight aligned wall sections. Here the dislocations of similar Burgers vector are arranged in single rows. Images showing such characteristic situation in mc-Si [34], deformed NaCl single crystals [35] and Bridgman-grown CdTe (figure 9). It is noteworthy that the origins and building mechanisms of both structures are somewhat differing. While the cellular patterns discussed in ch. 3.1 are priority based on the principle of dissipative structuring requiring glide and climb the sharp well-pronounced grain structure is formed by DP - a typical process of enthalpy minimization as it was discussed in detail in ch. 2. DP reduces the elastic deformation of the lattice planes by their splitting in similar oriented grains via movement of the stored dislocations into grain boundaries and their simultaneous annihilation. The determining mechanism is glide which can take place down to relative low temperatures. Thus, although both processes of pattern formation can start together at high temperatures only DP is still running down to moderate temperatures such as in solution and vapour bulk growth as well as epitaxial processes. To reduce the danger of polygonization and related low-angle grain structuring a strong homogenization of the temperature field within the cooling crystal is required. From technological point of view that means that the acting temperature gradients must be linearized as well as possible [36].

Note, there is also a totally different origin of formation of low-angle grain boundaries, which are not so easy to differentiate from DP in as-grown crystals. In case of morphological instabilities of the propagating melt-solid crystallization fronts caused by constitutional supercooling, characteristic cellular-shaped interfaces appear (middle figure 2). They produce columnar grain boundary patterns similar to polygonized cell structuring, because the growing-in dislocations are assembled by their line bending toward the concave cusps (i.e., along the column boundaries). This has been very clearly observed by real-time synchrotron X-ray topography on Al-0.73 wt% Cu alloy [37]. To prevent such type of structuring an optimum ratio between growth rate and temperature gradient at the interface must be maintained as has been described in many textbooks of crystal growth (e.g. ref. [38]).

It is important to note a further grain formation mechanism which is observed at epitaxial processes when after the nucleation a 3D (e.g. columnar or pyramidal) growth mode with subsequent coalescence takes place. For instance, at vapor growth of GaN layers on foreign substrates the coarsening of primarily nucleated GaN islands generates a low-angle grain structure that develops marked tensile stress as was explained by Nix and Clemens [39] (figure 10a). Due to the elastic displacement between the islands a biaxial strain is formed enhancing the bowing and even cracking of the growing layer. As was recently shown by Gorn et al. [22] in GaN films the dislocation-induced stress increases with increasing grain dimension (figure 10b). In ref. [39] was mentioned that high-mobility ad-atoms can help to relax such stress by their diffusion into the gaps between grains. However, a rapid lateral overgrowth mode would to be of more efficiency. Generally, such detailed studies of interplay between dislocation arrays and the related induced stress is an essential actual problem to obtain high-quality heteroepitaxial layers on various substrates.

3.3 Dislocation bunching

The clustering (bunching) of dislocations is a well-known harmful defect mode in as-grown and loaded crystals being a long-term subject of investigation. Such phenomenon is not only typical in dislocation containing semiconductor crystals, such as mc-Si, III-Vs and II-VIs, but also in metals, alloys and dielectrics. They are most intensively studied on metals under load having high dislocation densities. Usually, they are related to acting mechanical and thermomechanical stresses. However, they also correlate with polycrystallinity, i.e. the presence of

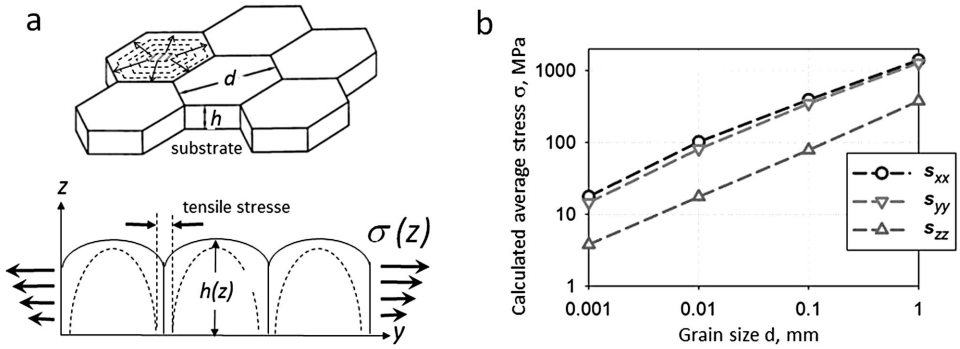

Fig. 10 Stress situations at epitaxial processes within the growing layers with grain boundary structure. a - sketch of a film after coalescence starting from regularly arranged nuclei with *h* the film height and *d* the grain diameter. At a certain gap between adjacent islands tensile stress components and an total elastic stress σ, associated with forming a continuous film, is obtained (adapted from ref. [39]); b - dependencies of the standard deviations from diagonal stress components s_{xx}, s_{yy}, s_{zz} on the average grain size *d* in GaN films (adapted from ref. [22]).

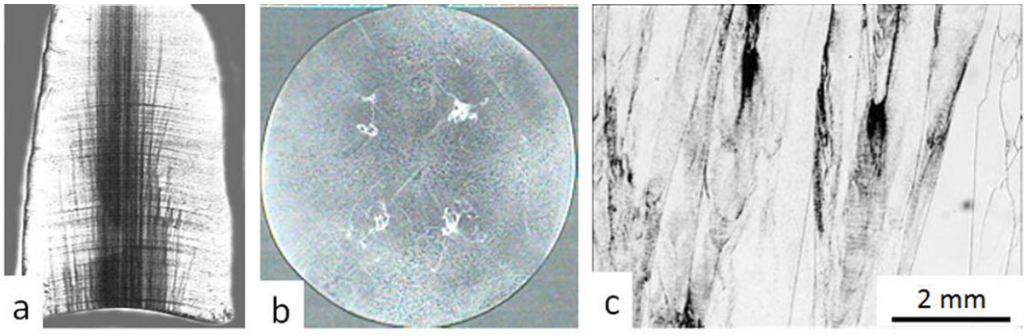

Fig. 11 Dislocation bunching. a - longitudinal 40 mm long plate cut from the center of a Czochralski salol crystal showing the dislocation bunching at concave melt-solid interface (adapted from ref. [16]); b - 4-inch GaAs Czochralski crystal grown with convex-concave melt-solid interface (author's collection); c - plate cut from a mc-Si ingot parallel to the crystallization direction (image by U. Juda from IKZ Berlin).

large-angle grain boundaries. Further, dislocation clustering can appear even in crystals with low defect density, especially, in case when foreign phase inclusions are presented. Dislocation bundles are also formed during crystallization if concave-convex and morphological instable melt-solid interfaces are presented (figure 11a, b). In sum, their appearance and origins are versatile and often of stochastic character making their prevention difficult.

For instance, in mc-Si ingots for photovoltaics (PV), crystallized by directional solidification (DS), dislocation clustering is a hotly debated object due to its continuous presence and harmfulness. About 10% of the surface area of commercially available mc-wafers are covered with such clusters of diameters between 0.1 and 1.0 mm containing dislocation densities of 10^6 - 10^8 cm^2 [40]. They degrade the minority carrier life and, hence, the solar cell efficiency by more than 3 - 4 percentage points [41]. Once they are formed mostly they follow the propagating solidification interface through the whole crystal remembering veins (figure 11c). Due to their gettering ability for highly diffusive metallic impurities the shorting of p-n-junctions is most likely. Therefore, their avoidance in solar cells is of highest priority.

Principally, one has to differ between i) hetero- or ii) homogeneously generated types of clustering. Type i) is formed around inclusions and is accompanied by a characteristic core of second phase. Contrary to that type ii) consists of a high number of pure tangled dislocations only [26, 42]. Today, the genesis of type i) defects is well understood from many melt and solution growth experiments [43]. Especially, during the solidification of compounds without stoichiometry control the excess component is incorporated as small *liquid inclusions* mostly generating marked misfit stress during solidification at their boundary to the matrix. As a result, a halo of high dislocation density is formed around the inclusion as it has been ascertained in many different crystals

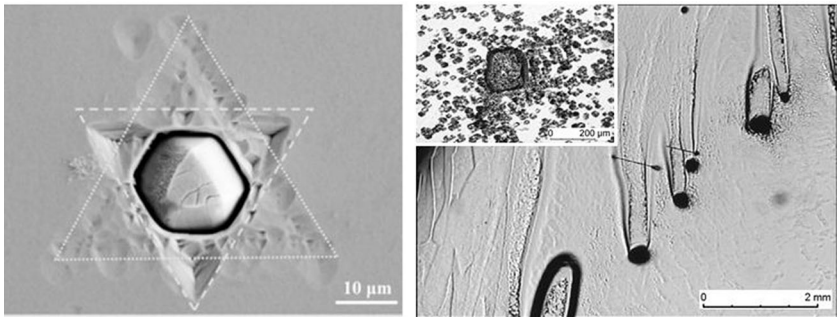

Fig. 12 Left - etch pits rosette surrounding a Te inclusion in Bridgman-grown (Cd,Zn)Te crystals (adapted from ref. [45]); right - dislocation clustering around Ga inclusions in a GaAs LEC crystal. The insert shows a magnified image (author's collection).

[44, 45] (figure 12a). For instance, Yadava [46] attributes the dislocation bundling around Te inclusions in CdTe crystals to the Greenwood–Foreman–Rimmer mechanism after what an interstitial dislocation loop punching takes place. The often observed star-like dislocation arrangement around the inclusion refers to such mechnisms. Due to the travelling solvent mechanisms the included micro droplets penetrate against the acting temperature gradient by releasing a trail with misfit dislocations (figure 12b).

Further, second-phase inclusions can also appear when in front of the growing interface an segregation-driven diffusion boundary layer is formed. If the therein enriched impurity concentration exceeds the solubility limit micro particles are nucleated and very likely incorporated [47]. Based on the theoretical treatment of Chernov and Tjemkin [48] first Fedorov [49] verficated experimentally that Ni micro-particles in salol are repulsed when the growth velocity is chosen undercritically. Friedrich et al. [50] studied the interaction of SiC particles with the moving solid-liquid interface during directional solidification of silicon. Even at growth velocities of 1 - 2 mm h^{-1}, being also typical for vertical gradient freezing (VGF) of various materials, foreign particles with diameters up to about 10 μm are incorporated. It was shown that the melt convection might cause a lift force which would push the particles away from the solid-liquid interface. Therefore, an prober mixing of the mother phase, e.g. by accelerated crucible rotation technique (ACRT) [51] or traveling magnetic fields (TMF) [52], proves to be very effective measure to minimize the second phase particle engulfment probability and, thus, one of the possible initiators of dislocation bunching. Recently a profound modelling review on the physical mechanisms determining the pushing or engulfment of a solid particle at a moving solid-liquid interface was published by Tao et al. [53].

Type ii) bunching is very often observed when concave fluid-solid interfaces [54] or crystallization fronts with regions of re-entrant angles (due to cellular morphology [37]) are acting during growth. The characteristic build-up at the concave-to-convex transition region has obviously to do with collision of dislocation glides along the basic glide system (figure 11b). Once they are formed they follow the propagating interface through the whole crystal (see figure 11a). Even a multi-grain interface, typical for crystallization of mc-Si ingots, consists of re-entrant corners (nooks) even between misoriented grains. In fact, the majority of the dislocations found in mc-Si are nucleated at grain boundaries close to the solid-liquid interface [40]. Even constitutional supercooling can generate cellular interface morphology with alternating vales. As was shown in ch. 2 the preferred dislocation propagation directions are mostly normal to the growing interface. Thus, at concave regions the dislocation lines are bended into the vale center forming here strung-out bundled veins which follow the crystallization front. Generally, it is proved experimentally by monocrystalline growth that bunching is reduced with flat-to-slightly-convex interface design without any concave parts.

When large-angle grain boundaries are presented dislocation pile-up can be obtained as has been listed in ch. 2. If a series of dislocations with the same Burgers vector all lying in the same slip plane meet such a hard obstacle like grain boundary mostly the dislocations pile-up behind the leading dislocation. A large long-range stress is produced at the head of the pile-up increasing with involved dislocation number. It can cause dislocation multiplication by cross slip of screw dislocations held up at obstacles such as precipitates and forming thus a dislocation gnarl. For instance, a near screw aggregation was ascertained at the grain boundary in mechanically loaded titanium [55]. The high-resolution electron backscatter diffraction revealed a maximum stress at the leading dislocation of 500 MPa much more than would demand for dislocation multiplication. Quite similar effect has been observed in mc-Si ingots [40, 56].

Another concept couples dislocation bunching in cyclically stressed metals with oscillating strain [57] leading to the question: could convective fluctuations play a similar affecting role at crystal growth? Further

studies are necessary to clarify this question. It is noteworthy that thermal, elastical and structural parameter fluctuations can play a crucial role. As was recently summarized by Kubin [8], the plastic flow is not uniform at a fine scale. The inhomogeneous release of elastic energy gives rise to the emission of *acoustic waves* (avalanches) interplaying with stored sessile dislocations and micro obstacles (e.g. precipitates). As a result in the course of cooling down sporadic clouded dislocation patterns are frozen up.

Thus, until today the complete elimination of type ii) dislocation clustering proves to be a particular challenge. Besides the careful prevention of constitutional supercooling, concave regions at the growing interface, grain boundaries and all kinds of obstacles within the crystal matrix the minimization and homogenization of the dislocation density are substantial counter methods. Note, from such point of view epitaxial processes using structured substrates with stripe masks or micro trench profile, being very helpful to minimize the misfit stress between GaN layers and sapphire, for example, prove to be quite problematically due to the artificially patterned dislocation bundling aligned parallel to the growth direction. For that it is helpful to change the growth mechanism towards a lateral overgrowth mode. For instance, high-quality heteroepitaxial GaN crystals can be obtained by facet controlled epitaxial lateral overgrowth (FACELO) [58]. Increasingly is also tested the two-step growth mechanism. After a first 3D island, preferably pyramidal growth mode that promotes the dislocation bending (see ch. 2), follows a 2D step-by-step overgrowth mechanism supporting the lateral growing out of dislocations [59]. However, as has been noted by Semond [60] such mode transition is still not problem-free because during the 3D growth the incorporation of impurities (e.g. oxygen) is enhanced.

3.4 Bundled dislocation glides

At the end of nineties the appearance of bundled dislocation glides during standard epitaxial MBE processes of (In,Ga)As layers on GaAs wafers exited the minds. Pseudo symmetric, four-fold set bundles of dislocations which start at the sample edges and glide into the bulk of the wafer following <110> glide line directions are formed at epitaxy temperatures around 600 °C (figure 13). The individual dislocations in the bundles are threading up through the epilayers impairing the devices made from. The X-ray transmission analysis showed that this phenomenon has nothing to do with lattice misfit but solely with thermal treatment induced plastic deformation

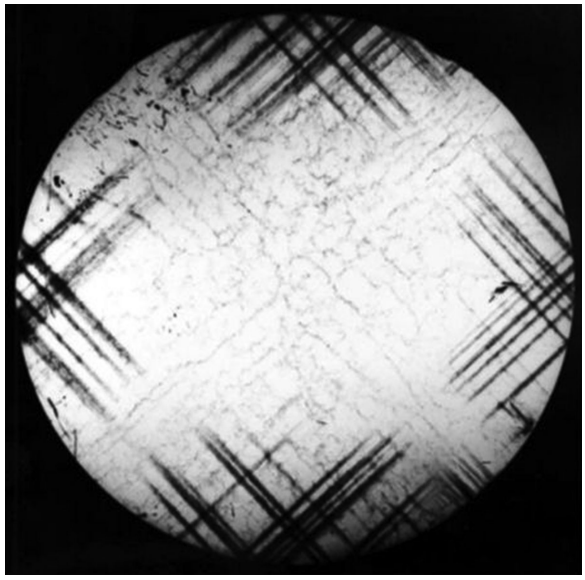

Fig. 13 X-ray transmission topogram [$(\bar{2}0\bar{2})$ reflection] of an epitaxial structure consisting of a basic VGF 2-inch (100)-oriented GaAs wafer, GaAs buffer layer, $In_{0.06}Ga_{0.94}As$ epilayer and GaAs capping layer growing by MBE at 600 °C (buffer layer) and 520 °C (epilayer). Parallel arranged dislocation bundles, starting at the sample edges and gliding along the <110> directions, are generated by plastic deformation in an inhomogeneous temperature field during epitaxy [61] (with permission of Wiley & Sons Ltd.).

[61]. Even temperature inhomogeneities across the area of the substrate holder are responsible for the formation of such slip lines [62, 63]. It is assumed that the nucleation of majority-type dislocation bundles took place as half-loops at surface irregularities at the wafer edge. After nucleation, the half-loops could have expanded by glide processes. Brochard et al. [64] showed that dislocation partials can appear from surface ripple troughs. Junqua and Grilhe [65] favor the nucleation of dislocations at surface steps that requires less energy than from a plane surface. Thus, it is of high technological importance to ensure an absolute temperature homogeneity across the substrate area during the whole epitaxy process.

In general, the deepening of the detailed knowledge on dislocation nucleation at crystal surfaces during each crystal growth process is recommended. For instance, a critical moment could be raised at growth of cylindrical bulk crystals showing often on their surface but also across a convex crystallization front microfacets forming fissured boundaries between them and atomically rough regions that may promote dislocation generation. To prevent such feature both the minimization of the dislocation-promoting thermo-mechanical stress and interface leveling are essential counter measures.

4 Conclusions

The most complicate structures of dislocation dynamics in as-grown crystals and epitaxial layers have been reviewed – dislocation patterning and bunching. First, phenomenologically the fundamentals of dislocation interactions have been outlined leading to various kinds of structuring. Both, thermodynamic equilibrium principles of enthalpy minimization and non-equilibrium dissipative structuring via irreversible thermodynamics are responsible for. Whereas dislocation screening, annihilation, dipole formation, dynamic polygonization and clustering are typical energy reducing processes the dislocation cell structuring can be assigned for the most part to the acting conditions of thermodynamical non-equilibrium such as permanent flows of heat, mass and stress being strictly speaking presented in each crystal growth process. Then, selected practical evidences of dislocation patterning and bunching in bulk and epitaxial crystals were reviewed. Various experimental counter measures, such as minimization of thermo-mechanical stress, leveling of the crystallization boundary, solution hardening, effective fluid mixing, stoichiometry control and lateral overgrowth at epitaxy have been shown. At the present, some features of dislocation dynamics are still not yet clarified in crystal growth processes. To solve this problem first of all a more intense *bridge between crystal growers and metal physicists dealing with dislocation patterning in solids* is highly recommended. Finally, more fundamental in situ experiments, such as high-temperature real-time synchrotron X-ray topography on elastically deformed crystallizing pieces, and application of advanced numeric modeling codes are necessary.

Acknowledgement. The author is very thankful to his former coworkers at the Leibniz-Institute of Crystal Growth in Berlin. Especially he is indepted to Ch. Frank-Rotsch, U. Juda, M. Naumann, F.-M. Kiessling, M. Neubert and M. Czupalla for their experimental works and useful discussions contributing to the study of dislocation dynamics in growing crystals. Also he like to thank the Freiberger Compound Materials (FCM) GmbH for supporting the investigations.

Key words. dislocation dynamics, cell structure, dynamic polygonization, dissipative structuring, bundling.

References

[1] M. M. Myshlyaev, Kristall und Technik **14**, 1185 (1979).
[2] S. V. Tsivinsky and L. A. Maslova, Kristall und Technik **15**, 1235 (1980).
[3] M. Ya. Dashevsky and M. Eeidenson, Kristall und Technik **14**, 29 (1979).
[4] E. Schmid, S. Würzner, C. Funke, Th. Behm, R. Helbig, O. Pätzold, H. Berek, and M. Stelter, Kristall und Technik **47**, 229 (2012).
[5] P. Rudolph, Kristall und Technik **14**, 29 (2005).
[6] B. Wu, S. Scott, N. Stoddard, R. Clark, and A. Sholapurwalla, in: TMS - The Minerals, (Metals & Materials Society, San Francisco, CA, USA 2009).
[7] W. Koch, A. L. Endrös, D. Franke, C. Häßler, J. P. Kalejs, and H. J. Möller, in: Handbook of Photovoltaic Science and Engineering, Eds: A. Luque and S. Hegedusp, (John Wiley & Sons, Weinheim 2005), ch. 6, p. 205
[8] L. P. Kubin, Dislocations, Mesoscale Simulations and Plastic Flow, (Oxford University Press, Oxford 2013).
[9] R. J. Amodeo and N. M. Ghoniem, Physical Review B **41**, 6958 and 6968 (1990).
[10] M. Soleymani, M. H. Parsa, H. Mirzadeh, Computational Materials Science **84**, 83 (2014).
[11] M. Peach and J. S. Koehler, Phys. Rev. **80**, 436 (1950).
[12] G. A. Malygin, Phys Solid State **44**,1305 (2002), transl. russ. Fiz. Tverd. Tela 44, 1249 (2002).
[13] A. N. Gulluoglu, D. J. Srolovitz, R. LeSar, and P. S. Lomdahl, Scripta Metallurgica **23**, 1347 (1989).
[14] D. Hull and D. J. Bacon, Introduction to Dislocations, Fith ed., (Elsevier, Amsterdam 2011).
[15] M. Tang, G. Xu, W. Cai, and V. Bulatov, Mat. Res. Soc. Symp. Proc. **795**, U2.4.1 (2004).
[16] H. Klapper, in: Springer Handbook of Crystal Growth, Eds. G. Dhanaraj, K. Byrappa, V. Prasad and M. Dudley, (Springer, Heidelberg 2010), ch. 4, p. 93.
[17] P. Vennégués, B. Beaumont, V. Bousquet, M. Vaille, and P. Gibart, J. Appl. Phys. **87**, 4175 (2000).
[18] B. Billia and R. Trivedi, in: Handbook of Crystal Growth Vol **IB**, Ed. D. T .J. Hurle, (North-Holland, Amsterdam 1993), ch. 14, p. 899.
[19] M. Zaiser, in: Crystal Growth - from Theory to Technology, Eds. G. Müller, J. Metois and P. Rudolph, (Elsevier, Amsterdam 2004), ch. 2, p. 215.
[20] D. Walgraef and E. C. Aifantis, Int. J. Engng. Sci. **23**, 1351 (1985).
[21] J. F. Nye, Acta Metallurgica **1**, 153 (1953).
[22] N. L. Gorn, D. V. Berkov, and M. Jurisch, Abstracts of 1-st German Czechoslovak Confernce on Crystal Growth (GCCCG-1/DKT2016), March 16-18, 2016, Dresden, p. 84.
[23] S. V. Raj and G. M. Pharr, Mat. Sci. Eng. **81**, 217 (1986).
[24] G. Grange, C. Jourdan, A. L. Coulet, and J. Gastaldi, J. Crystal Growth **72**, 748 (1985).
[25] B. Jakobson, H. F. Poulsen, U. Lienert, J. Almer, S. D. Shastri, H. O. Sørensen, C. Gundlach, and W. Pantleon, Science **312**, 889 (2006).
[26] P. Rudolph, Ch. Frank-Rotsch, U. Juda, M. Naumann, and M. Neubert, J. Crystal Growth **265**, 331 (2004).
[27] P. Rudolph, Ch. Frank-Rotsch, U. Juda, and F.-M. Kiessling, Mat. Science and Engineering A **400–401**, 170 (2005).
[28] Ch. Frank-Rotsch, U. Juda, F.-M. Kiessling, and P. Rudolph, Mat. Sci. Technol. **21**, 1450 (2005).

[29] D. Holt, J. Appl. Phys. **41**, 3197 (1970).
[30] N. Miyazaki, in: Handbook of Crystal Growth, Second Edition, Vol **IIB**, Ed. P. Rudolph, (Elsevier, Amsterdam 2015), ch. 26, p. 1049.
[31] J. P. Poirier, Creep of crystals - high-temperature deformation processes in metals, ceramics, (Cambridge Earth Science Series, Cambridge University Press, Cambridge 1985).
[32] P. Rudolph and F.-M. Kiessling, J Cryst Growth **292**, 532 (2006).
[33] B. Bako, I. Groma, G. Györgyi, and G. Zimanyi, Comp. Mater. Sci. **38**, 22 (2006).
[34] T. Ervik, M. Kivambe, G. Stokkan, B. Ryningen, and O. Lohme, Acta Mater. **60**, 6762 (2012).
[35] S. V. Raj and G. M. Pfarr, Mater. Sci. Eng. **A122**, 233 (1989).
[36] V. L. Indenbom, Kristall u. Technik **14**, 493 (1979).
[37] G. Grange, C. Jourdan, J. Gastaldi, and B. Billia, J. Phys. France **4**, 293 (1994).
[38] W. A. Tiller, The Science of Crystallization - Macroscopic Phenomena and Defect Generation, (Cambridge University Press, Cambridge 1992).
[39] W. D. Nix and B. M. Clemens, J. Mater. Res. **14**, 3467 (1999).
[40] B. Ryningen, G. Stokkan, M. Kivambe, T. Ervik, and O. Lohne, Acta Mat. **59**, 7703 (2011).
[41] B. Sopori, C. Li, S. Narayanan, and D. Carlson, Mater. Res. Soc., Symp. Proc **864**, 233 (2005).
[42] M. Naumann, P. Rudolph, M. Neubert, and J. Donecker, J. Crystal Growth **231**, 22 (2001).
[43] H. Klapper and P. Rudolph, in: Handbook of Crystal Growth, Second Edition, Vol **IIB**, Ed. P. Rudolph, (Elsevier, Amsterdam 2015), ch. 27, p. 1093.
[44] P. Rudolph, A. Engel, I. Schentke, and A. Grochocki, J. Crystal Growth **147**, 297 (1995).
[45] Yadong Xu, Yihui He, Tao Wang, Rongrong Guo, Wanqi Jie, P. J. Sellin, and M. Veale, Cryst. Eng. Comm **14**, 417 (2012).
[46] R. D. S. Yadava, R. K. Badai, and W. N. Borle, J. Electron. Mater. **21**, 1001 (1992).
[47] A. K. Søiland, E. J. Øvrelid, T. A. Engh, O. Lohne, J. K. Tuset, and Ø. Gjerstad, Mat. Sci. in Semicond. Processing **7**, 39 (2004).
[48] A. A. Chernov and D. E. Temkin, in: Current Topics of Materials Science: Crystal Growth and Materials, Vol. **2**, Eds. E. Kaldis and H. J. Scheel, (North-Holland, Amsterdam 1977), p. 3.
[49] O. P. Fedorov, J. Cryst. Growth **102**, 857 (1990).
[50] J. Friedrich, C. Reimann, T. Jauss, A. Cröll, and T. Sorgenfrei, J. Crystal Growth **447**, 18 (2016).
[51] H. Scheel, J. Crystal Growth **13-14**, 560 (1972).
[52] P. Rudolph, J. Crystal Growth **310**, 1298 (2008).
[53] Y. Tao, A. Yeckel, and J. J. Derby, J. Crystal Growth (2016) (in press), electron. version: http://dx.doi.org/10.1016/j.jcrysgro.2015.12.037
[54] M. Shibata, T. Suzuki, S. Kuma, and T. Inada, J. Crystal Growth **128**, 439 (1993).
[55] T. B. Britton and A. J. Wilkinson, Acta Materialia **60**, 5773 (2012).
[56] D. Oriwol, E.-R. Carl, A. N. Danilewsky, L. Sylla, W. Seifert, M. Kittler, and H. S. Leipner, Acta Materialia **61**, 6903 (2013).
[57] O. Politano and J. M. Salazar, Mat. Si. Eng. **309-310**, 261 (2001).
[58] P. Hofmann, C. Röder, F. Habel, G. Leibiger, F. C. Beyer, G. Gärtner, S. Eichler, and T. Mikolajick, J. Physics D: Applied Physics **49**, 075502 (2016).
[59] L. Ying-Ying, Z. Jun, L. Wen-Bo, H. Lan-Zhong, Z. Ying, and L. Yan-Rong, Chin. Phys. B **20**, 108102 (2011).
[60] F. Semond, MRS Bulletin **40**, 412 (2015).
[61] P. Möck, J. Appl. Crystallography **34**, 65 (2001).
[62] M. Yamada, M. Fukuzawa, and K. Ito, Inst. Phys. Conf. Ser.No. **155**, 901 (1997).
[63] S. Sawada, H. Yoshida, M. Kiyama, H. Mukai, R. Nakai, T. Takebe, M. Tatsumi, M. Kaji, and K. Fujita, Technical Digest–IEEE GaAs Integrated Circuit Symp. **74**, 50 (1996).
[64] S. Brochard, N. Junqua, and J. Grilhé, Phil. Mag. A **77**, 911 (1998).
[65] N. Junqua and J. Grilhé, Phil. Mag. Lett. **75**, 125 (1997).

